EURATOM

Project Deliverable

Project number:	Project Acronym:	Project title:
212246	SEDENTEXCT	Safety and Efficacy of a New and Emerging Dental X-ray Modality

Instrument:	Activity code:
Collaborative Project (Small or medium-scale focused research project)	Fission-2007-3.2-01

Start date of project:	Duration:
1 January 2008	42 months

Title:
D2.3: Determination of effective dose and conversion factors for wide range of operating conditions in representative sample of commercially available CBCT equipment

Contractual Delivery date:	Actual Delivery date:
1st January 2011	V1.0: 24th March 2011 V1.0 (public): 8th June 2011

Organisation name of lead beneficiary for this Deliverable:	Document version:
KUL Katholieke Universiteit Leuven	V1.0 (public)

Dissemination level:		
PU	Public	X
PP	Restricted to other programme participants (including the Commission)	
RE	Restricted to a group defined by the consortium (including the Commission)	
CO	Confidential, only for members of the consortium (including the Commission)	

Authors (organisations):

Keith Horner (UNIMAN): SEDENTEXCT Co-ordinator
Ria Bogaerts (KUL): WP2 Lead
Ruben Pauwels (KUL)
Anne Walker (UNIMAN)
Chrysoula Theodorakou (UNIMAN)

Abstract:

This is a public version of deliverable D2.3, and excludes some material not yet ready for the public domain.

In this final deliverable for WP2, the different work package tasks are combined to determine an effective dose range for a wide range of CBCT devices, as well as conversion factors between dose simulations, dose indices and patient risk.

Three major tasks were performed. The effective dose was experimentally determined for a wide range of CBCT devices and protocols, using adult and paediatric anthropomorphic phantoms. Using a customised PMMA phantom, the dose indices defined in deliverable 2.1 were measured in practice for different CBCT exposure geometries. Conversion factors to effective doses were calculated using Monte Carlo simulations, for a number of devices, exposure protocols and phantoms.

The combined information from these three tasks led to the determination of an effective dose range for CBCT and the determination of correlation and conversion factors between dose index and patient effective dose.

Table of Contents

1. Executive summary

This deliverable combines three tasks performed in WP2: the measurement of the absorbed organ dose and effective dose in anatomical phantoms, (WP2.2), the validation of a standardised dose index (WP2.1) and the development and validation of a Monte Carlo simulation framework for dental CBCT dosimetry (WP2.4).

Deliverable 2.1 contained effective dose measurements for adult and paediatric phantoms, involving a wide range of CBCT devices and protocols. After completion of D2.1, additional measurements were obtained for the adult, adolescent and 10 year old phantom. This concludes the assessment of organ and effective doses in dental CBCT using experimental measurements.

Another task which was represented in D2.1 was the definition of a specific standardised dose index for dental CBCT, based on the measurement of dose distribution for all possible exposure geometries used by CBCT devices in practice. The indices defined in D2.1 were measured on two CBCT devices using a customised PMMA phantom provided by Leeds Test Objects. All possible exposure geometries (field of view size, positioning of the field and rotation arc) were explored.

A third, major task was the set-up of a simulation framework to simulate CBCT exposures using the Monte Carlo code. A large number of CBCT devices and phantoms were modelled on a validated Monte Carlo framework, and conversion factors were determined to obtain the effective dose from these simulations. Furthermore, the relation between these simulated effective doses and the measured dose indices was investigated.

2. The Context

2.1 SEDENTEXCT aims and objectives

The aim of this project is the acquisition of the key information necessary for sound and scientifically based clinical use of dental Cone Beam Computed Tomography (CBCT). In order that safety and efficacy are assured and enhanced in the 'real world', the parallel aim is to use the information to develop evidence-based guidelines dealing with justification, optimisation and referral criteria and to provide a means of dissemination and training for users of CBCT. The objectives and methodology of the collaborative project are:

1. To develop evidence-based guidelines on use of CBCT in dentistry, including referral criteria, quality assurance guidelines and optimisation strategies. Guideline development will use systematic review and established methodology, involving stakeholder input.

2. To determine the level of patient dose in dental CBCT, paying special attention to paediatric dosimetry, and personnel dose.

3. To perform diagnostic accuracy studies for CBCT for key clinical applications in dentistry by use of in vitro and clinical studies.

4. To develop a quality assurance programme, including a tool/tools for quality assurance work (including a marketable quality assurance phantom) and to define exposure protocols for specific clinical applications.

5. To measure cost-effectiveness of important clinical uses of CBCT compared with traditional methods.

6. To conduct valorisation, including dissemination and training, activities via an 'open access' website.

At all points, stakeholder involvement will be intrinsic to study design.

2.2 Work package 2 (WP2) objectives

It is fundamental to radiation protection that the benefits of a procedure using ionizing radiation outweigh the risks; this is incorporated into the relevant European Directive 97/43/Euratom. The limited studies in the literature indicate that the radiation dose achievable with CBCT units is substantially less than conventional CT but higher than conventional dental imaging. In addition the radiation dose varies according to the particular manufacturer's system being assessed. For example, one system may give a dose ten times another for the same examination. Doses are many times greater than those for conventional 'dental' examinations. Dose depends upon the size of the volume of the patient imaged and the other selected technique factors.

These studies suffer because they are individually limited to reports related to one or two CBCT systems. More work is needed to verify this limited literature on a greater range of current CBCT systems and without the inter-study variation in measurement methodologies; the research will achieve this. Importantly, however, our research specifically deals with paediatric dosimetry, an area that has not been previously assessed using anatomically appropriate paediatric phantoms. Our research also develops a robust system of Monte Carlo dose simulation for CBCT that will facilitate optimisation of exposures.

The overall aim of this work package is to determine the level of (1) patient dose in dental CBCT, paying special attention to paediatric dosimetry, and (2) personnel dose. These goals correspond to the following sub-objectives:

1. To develop a method to readily characterise the dose distribution for different scanners, using measurements simply performed in the field, to allow simple conversion to effective dose.

2. To determine the scatter dose distribution around scanners and explore the consequences for operator dose.

2.3 Anticipated impact of the work

This section describes the impact of the work in this Work Package as anticipated at the start of the project.

For almost a decade, the use of CBCT in dental practice has been increasing rapidly. It is now the modality of choice for the planning of dental implant surgery, and it is used for many additional dental applications such as endodontics, orthodontics and maxillofacial surgery. CBCT allows for the imaging of the dentomaxillofacial area in three dimensions at a relatively low radiation dose compared to MSCT. However, pilot studies have shown that doses for CBCT are still significantly higher than those for conventional, two-dimensional modalities (panoramic and cephalometric imaging). Furthermore, a larger number of CBCT devices have hit the market, exhibiting a wide range of exposure parameters.

A wide-scale dosimetric study was needed to accurately assess the radiation dose for a range of CBCT devices using standardized protocols. The different tasks within WP2 have provided a vast amount of dosimetric data, greatly increasing the knowledge of radiation dose in CBCT. The effect of different exposure parameters on patient dose was assessed, and can be related to image quality parameters measured within WP3 and WP4. Furthermore, a thorough investigation of the dose distribution has led to the definition and validation of different specific dose indices. Additional information was obtained through *in vivo* skin measurements and Monte Carlo simulations, and conversion factors were defined to relate a technical dose index to the effective dose.

The impact of the research performed within WP2 is twofold: a number of journal papers that are currently in press, in review or planned for submission will inform the research community about the different aspects of CBCT radiation dose, and will provide all the necessary information for the optimisation of patient and personnel dose. The research will also be incorporated into the SEDENTEXCT Guidelines, providing different dose limitation strategies. Also, the dosimetric work feeds into the QA protocol of WP3, as part of it encompasses radiation dose. Furthermore, a customized phantom was defined, enabling the measurement of two dose indices which can be used for device intercomparison, dose optimization or quality control.

Table 1. Anticipated impact for different stakeholder groups

Stakeholder(s)	**Impact**
Research community	Journal papers published or planned on: • Adult effective dose • Paediatric effective dose • Dose distribution for the purpose of defining a dose index • Validation of potential dose indices • Determination of conversion factors • Skin dose measurements • Scatter (personnel) dose
Radiologists Medical physicists Dentists	Dosimetric knowledge incorporated into guidelines and QA protocol, enabling the optimization of radiation dose by all users of CBCT equipment, and quality control of devices. Definition of a customized cylindrical PMMA phantom, which can be used by medical physicists as a quality control tool.
Patients Personnel	Limitation of patient and occupational dose.

2.4 Current state of the art

It is fundamental to radiation protection that the benefits of a procedure using ionizing radiation outweigh the risks; this is incorporated into the relevant European Directive 97/43/Euratom. To measure the radiation risk for patients from a radiographic modality, the effective dose is still accepted as the most suitable parameter. There have been a number of studies measuring the effective dose on dental CBCT using thermoluminescent dosimeters (TLDs) in combination with a human phantom [Loubele *et al*, Ludlow *et al*, Okano *et al*, Suomalainen *et al*, Silva *et al*, Tsiklakis *et al*, Roberts *et al*, Hirsch *et al*]. These studies provide some estimation of the range of doses that are obtained from these devices, but are not comparable, seeing that different types of phantoms are used as well as different TLD positioning schemes, with the number of TLDs applied to the different organs often being too low for an accurate and reproducible estimation of the organ and effective doses. Besides, there have been no studies assessing the paediatric effective dose for dental CBCT examinations.

Furthermore, the effective dose cannot be directly applied to a patient, and some consideration is needed when using this quantity to estimate patient risk. Dental CBCT involves different patient groups, showing a wide age range. It is clear that the actual dose received by different subsets of patients can vary to a great extent, depending on patient size and mass. By performing *in vivo* skin dose measurements on patients, the range of actual doses can be determined, but no studies have involved skin dose measurements for dental CBCT.

Regarding the use of a standardized dose index in dental CBCT, the use of the computed tomography dose index (CTDI) has been under investigation lately for both CBCT and MSCT [Jessen *et al*, Dixon 2003, Mori *et al*, Nakonechny *et al*, Lofthag-Hansen *et al*, Brenner *et al*, Dixon 2006, Dixon and Boone, Fearon]. It is clear that MSCT and CBCT are similar to some extent regarding the geometry of the exposure, and the classical CTDI is not applicable to either modality. However, dental CBCT provides a few additional (geometrical, anatomical and practical) issues that need to be taken into account before adapting or defining a suitable dose index. No studies have investigated the complicated dose distribution for dental CBCT devices.

Finally, there are no extensive reports available regarding the personnel dose for personnel using CBCT equipment. There are no clear guidelines regarding the proper installation of CBCT devices into dental practices or hospitals to limit the dose to the environment.

2.5 Deliverable D2.3

Deliverable D2.3 is the final deliverable of SEDENTEXCT Work Package 2. The objects of deliverable D2.3 are:

- To summarise earlier work
- To describe new work in this Work Package in the last period. The purpose of this work is the determination of effective dose and conversion factors for a wide range of representative CBCT devices and exposure protocols
- To describe the possible impact of work in this Work Package
- To outline dissemination plans and possible future work

Deliverable 2.3 presents effective dose measurements and conversion factors for a range of CBCT machines and exposure conditions. In addition, the validation results of the proposed dose indices, described in Deliverable 2.1, and the relationship between the dose indices and the effective dose is investigated.

During each x-ray examination, the patient is exposed to ionising radiation and thus, receives a dose. The adverse effects of radiation can be grouped into two categories, the deterministic and the stochastic effects. The deterministic effects, such as skin erythema and cataract, are due to the killing/malfunction of cells following high doses. There is a dose threshold below which the probability is zero. The lowest threshold is 0.5Gy for cataract formation, a dose which is orders of magnitude higher than the doses involved in dental CBCT examinations. Stochastic effects, i.e. cancer and hereditary effects are due to mutation of somatic cells or reproductive cells. There is no dose threshold for stochastic effects and even a small amount of radiation as in dental CBCT has a probability of inducing cancer. As there is always a risk for radiation-induced cancer or hereditary effects, the dose to the patient should always be as low as reasonably achievable (ALARA). This is the optimisation principle of the International Commission on Radiological Protection (ICRP), which was first precisely defined in ICRP 26 and has been part of the European Basic Safety Standards since 1980. In diagnostic radiology it means that the dose should be as low as possible, which is consistent with the required image quality and necessary for obtaining the desired diagnostic information.

The ICRP 103 recommended quantity for stochastic effects is the effective dose. The effective dose is the sum of the equivalent doses over all organs and tissues, weighted for their radiosensitivity. The equivalent doses are absorbed doses weighted for the relative biological effectiveness of the type of radiation. Therefore, the effective dose is weighted for the relative biological effectiveness of the different types of radiation and for the radiosensitivity of each tissue. The relative biological effectiveness of the radiation is expressed with the radiation weighting factor w_R which for photons is 1. The tissue radiosensitivity is expressed with the tissue weighting factors w_T (Table 1), which represent mean values for humans averaged over both sexes and all

ages. Thus, they do not correlate to the characteristics of a particular individual.

Table 2. ICRP 103 tissue weighting factors

Tissue	Tissue weighting factor w_T
Bone-marrow (red), colon, lung, stomach, breast, remainder tissues[a]	0.12
Gonads	0.08
Bladder, oesophagus, liver, thyroid	0.04
Bone surface, brain, salivary glands, skin	0.01
Total	1

[a] *Remainder tissues: Adrenals, extrathoracic (ET) region, gall bladder, heart, kidneys, lymphatic nodes, muscle, oral mucosa, pancreas, prostate (♂), small intestine, spleen, thymus, uterus/cervix (♀).*

The radiosensitive organs that are relevant to dental cone beam CT - since they are located in the head and neck region - are the red bone marrow, oesophagus, thyroid, brain, skin, endosteum (bone surface), salivary glands, extrathoracic region, lymphatic nodes, muscle and oral mucosa.

The effective dose cannot be measured directly on humans as it requires the determination of organ doses. There are two methods of indirectly estimating the effective dose. The first is by using computational methods and human voxel models and the second method involves dose measurements on anthropomorphic tissue equivalent phantoms. Both methods use phantoms or computational models that closely resemble a typical reference male or female as defined by ICRP 23. A complete exploration of the relationship between the effective dose and the exposure parameters, types of machines and clinical examinations could be limited using experimental methods because of time constraints posed by accessing the machines and handling the phantoms and dosimeters. Modelling, even though it is less accurate than measurements, overcomes the time limitations set by the experimental methods and by setting up a complete simulation environment, the relationship between the effective dose and the exposure parameters, types of machines, clinical examinations and conversion factors could be thoroughly investigated and quantified.

Since dental CBCT technology has recently been introduced in clinical practice there are only few studies that have attempted to estimate the doses in dental CBCT [Loubele *et al*, Ludlow *et al*, Okano *et al*, Suomalainen *et al*, Silva *et al*, Tsiklakis *et al*, Roberts *et al*, Hirsch *et al*]. All studies have focused on estimating the effective doses on adults and most of the studies measured doses for a limited number of machines using different phantoms and dosimeters making a dose intercomparison difficult. In addition, some of the studies used a limited number of dosimeters per organ without having assessed the uncertainty in the effective dose estimation.

In order to overcome the limitations of the published studies and to obtain a better picture of the range of effective doses involved in dental CBCT, this work has used both approaches to effective dose estimation. The first part of this report presents the experimental approach, i.e. measurements using adult and paediatric anthropomorphic tissue equivalent phantoms and thermoluminescent dosimeters for a range of dental CBCT machines and typical examinations. The second part presents the conversion factors to effective dose, which were calculated using computational methods, for a wide range of CBCT machines, examinations and exposure conditions.

2.6 Glossary

Absorbed dose: measure of the energy deposited in a medium by ionizing radiation. It is equal to the energy deposited per unit mass of medium (unit: J/kg, or Gray (Gy)).

CTDI: commonly used radiation exposure index in X-ray computed tomography.

Effective dose: quantity to estimate the whole-body stochastic risk (carcinogenesis and hereditary effects) of an exposure to ionizing radiation, taking the radiosensitivity of different tissues into account.

FOV: field of view, the total (most commonly cylindrical) volume that is included in a reconstructed CBCT scan.

Ionisation chamber: type of radiation dosimeter, collecting ion pairs from gases. A large variety of sizes and shapes of chambers are used for different applications.

Isocentre: centre of rotation of X-ray tube and detector, also the central point of the reconstructed scan.

kVp: voltage peak applied between the cathode and anode in an X-ray tube, determines the peak energy of the X-rays in a beam.

mAs: product of X-ray tube anode current and exposure time, determines the number of X-ray photons during a scan.

Off-axis scanning: situation where the central point of the FOV (isocentre) does not coincide with the centre of the scanned object.

Phantom: in this case, a geometrical or anthropomorphic test object used for the assessment of radiographic devices.

Monte Carlo simulations: a computational algorithm that can be used to model an imaging chain and simulate images and radiation dose.

TLD: Thermoluminescent dosimeter, a type of radiation dosimeter using a small crystal that captures the energy absorbed from X-rays.

3. Earlier work in WP2

WP2.1 Development of a standardised dose index to characterise dose distribution in CBCTs

The aim of WP2.1 was to characterise the dose distribution for a range of CBCT units, investigating different field of view sizes, central and off-axis geometries, full or partial rotations of the x-ray tube and different clinically applied beam qualities. The implications of the dose distributions on the definition and practicality of a dose index were assessed.

Based on the dose distribution measurements, different possible dose indices were presented. The proposed indices all provide an estimation of the dose which is deposited throughout a head-sized volume, and can be implemented into practice providing the appropriate equipment (phantom & dosimeter) are available.

Deliverable 2.1 contains the dose distribution measurements and definitions of the dose indices. Practical validation of the indices and the determination of conversion factors for effective dose are covered in the current deliverable.

WP2.2 Measurement of the dose distribution in anatomical phantoms and subsequent calculation of effective dose

The objective of this WP task was to estimate the absorbed organ dose and effective dose for a wide range of cone beam computed tomography scanners, using different exposure protocols and geometries. An adult phantom was used, as well as two (10 year old and adolescent) paediatric phantoms.

For the adult phantom, the effective dose for different CBCT devices showed a 20-fold range (19-368 µSv). The largest contributions to the effective dose were from the remainder tissues (37%), salivary glands (24%), and thyroid gland (21%). For all organs, there was a wide range of measured values apparent, due to differences in exposure factors, diameter and height of the primary beam, and positioning of the beam relative to the radiosensitive organs.

For the 10 year old and adolescent phantom, average effective doses were 116 µSv and 79 µSv respectively which are comparable to adult doses. Similar to the adult phantom, a wide range in effective dose was observed. The salivary glands received the highest dose and there was a fourfold increase in the thyroid dose of the 10 year old compared with the adolescent because of its smaller size. The remainder tissues, salivary and thyroid glands contributed the most to the effective dose for a 10 year old while for an

adolescent, the remainder tissues and the salivary glands contributed the most.

The results show that a distinction is needed between small-, medium-, and large-field CBCT scanners and protocols, as they are applied to different indication groups, the dose received being strongly related to field size. Furthermore, the dose should always be considered relative to technical and diagnostic image quality, seeing that image quality requirements also differ for patient groups. The results from the current study indicate that the optimisation of dose should be performed by an appropriate selection of exposure parameters and field size, depending on the diagnostic requirements. Furthermore, it was concluded that it is imperative that dental CBCT examinations on children should be fully justified over conventional X-ray imaging and that dose optimisation by field of view collimation is particularly important in young children.

WP2.3 In vivo dose measurements

In addition to phantom TLD measurements, skin dose measurements were undertaken for different scanner types and completed by M24 (Milestone 2.3). The skin dose measurements were performed in adult as well as paediatric patients, using clinical indications as identified in WP5.

A total of 248 patients were included in this study, encompassing six CBCT devices and a large number of exposure protocols, based on the clinical indication. A wide range of skin dose results was seen, due to patient factors (size and constitution) and scanning factors (FOV size and position, beam quality, amount of exposure).

These results aid in the establishment of diagnostic reference levels for dental CBCT, and provide further evidence that dose limitation is crucial for paediatric patients, and that the exposure should not be fixed but based on patient size.

WP2.4 Development of mathematical models for dental CBCT dosimetry

All work for WP2.4 is covered in the current deliverable.

WP2.5 Measurements of scatter dose and radiation protection of personnel and helpers

Scatter dose measurements were performed on ten different models of CBCT devices. The measurements were collected using two techniques: one active where a scattering material was placed in the CBCT and a radiation detector positioned at various locations in the room to measure during the exposure; the other passive where small dosimeters were attached to walls around the

CBCT for a period of 3 to 12 weeks while normal, clinical and non-clinical, exposures were performed.

Information was also gathered on the average number of patients seen in different CBCT facilities and the national requirements or guidelines on the design of such facilities with respect to radiation protection. Example calculations of the shielding requirements, combining all the data, were offered and recommendations based on the measurements were proposed.

4. Work in the Final Period: Methodology

Sections 4, 5 and 6 of this deliverable report the work in WP2 in the last period. The purpose of this work is the determination of effective dose and conversion factors for a wide range of representative CBCT devices and exposure protocols. This section describes how the work was performed.

4.1 Measurements using anthropomorphic equivalent phantoms

In Deliverable D2.1, measurements on anthropomorphic (adult and paediatric) phantoms were presented. These measurements were incorporated into D2.1 because they provided information on the effective dose for CBCT and the parameters that affect it (*e.g.* FOV size and positioning). However, for this deliverable, these measurements are crucial as well, as they are used to establish conversion factors between dose index and patient risk.

Furthermore, a number of additional effective dose measurements were performed in the second half of the SEDENTEXCT project to fill in certain gaps. This deliverable contains the results depicted in D2.1 as well as these additional measurements. The methodology for the measurements was described in D2.1, but a short overview is hereby provided. The methodology and results were adapted from two SEDENTEXCT papers that are currently in press: (1) Pauwels R *et al*. Effective dose range for dental cone beam computed tomography scanners. European Journal of Radiology; (2) Theodorakou C *et al*. Estimation of paediatric organ and effective doses from dental cone beam computed tomography using anthropomorphic phantoms. British Journal of Radiology.

To estimate the effective dose for an average adult male, two similar types of anthropomorphic male Alderson Radiation Therapy (ART) phantoms (Radiology Support Devices Inc., CA, USA) were used. They represent an average man (175 cm tall, 73.5 kg) and consist of a polymer mould simulating the bone, embedded in soft tissue equivalent material. They are transsected into 2.5 cm thick slices, each containing a grid for TLD placement. The phantoms were scanned on a variety of available CBCT devices, combining different exposure protocols when possible. The phantoms were positioned as closely as possible as a typical patient with the help of local radiographic staff using the positioning aids provided for the scanner. The following CBCT devices were included: 3D Accuitomo 170, GALILEOS Comfort, i-CAT Next Generation, Iluma Elite, Kodak 9000 3D, Kodak 9500, NewTom VG, NewTom VGi, Pax-Uni3D, Picasso Trio, ProMax 3D, SCANORA 3D, SkyView, Veraviewepocs 3D.

For paediatric effective dose estimations, two tissue-equivalent anthropomorphic phantoms (ATOM Model 702-C and ATOM Model 706-C, Computerized Imaging Reference Systems Inc, Norfolk, USA) were used.

Models 706-C and 702-C simulate a 10 year old child and an adult female respectively. An adult female phantom was used to simulate an adolescent patient as there are no commercially available adolescent anthropomorphic phantoms. The ICRP 89 reference values for body height for a 15 year old male and female are 167cm and 161cm respectively compared to 160cm of the female ATOM phantom. The weight of the female ATOM phantom is 55kg compared to ICRP 89 reference weight values 56kg and 53 kg for a 15 year old male and female respectively. The ATOM phantom design is based on ICRP 23 and ICRU 48 and available anatomical reference data. The tissue simulated in the ATOM phantoms are average bone and soft tissue, cartilage, spinal cord, spinal disks, lung, brain, sinus, trachea and bronchial cavities. The density of the simulated paediatric bone is typical of the age. The bone tissue is an average of known cortical to trabecular ratios and age based mineral densities.

The paediatric phantoms were scanned on a number of CBCT devices, using different exposure protocols where possible. In addition, MSCT, panoramic and cephalometric measurements were obtained to allow a comparison with these alternative modalities.

The following calculation was used to determine the equivalent dose or radiation weighted dose H_T for all organs or tissues T:

$$H_T = w_R \Sigma_i f_i D_{Ti}$$

In this formula, w_R is the radiation weighting factor (being 1 for X-rays), f_i the fraction of tissue T in slice i, and D_{Ti} the average absorbed dose of tissue T in slice i, the summation being over all slices.

In order to calculate the contribution E_T of each organ to the effective dose, the equivalent dose is multiplied by the tissue weighting factor w_T, which expresses the contribution of this tissue to the overall radiation detriment from stochastic effects:

$$E_T = w_T H_T \quad (1)$$

The tissue weighting factors that are defined in the latest recommendations of the International Commission on Radiological Protection were applied. The effective dose is calculated by taking the sum of the contribution E_T for all relevant organs. The oesophagus was originally included in the calculation, but it was found that this organ does not provide a significant contribution to the effective dose.

4.2 Dose index validation measurements

For the measurement of the two indices proposed in D2.1, a new customized cylindrical PMMA phantom was created by Leeds Test Objects. This phantom enables ion chamber measurements at central and different peripheral

locations (Figure 1). TLD and film measurements are also possible but were not needed for dose index validation.

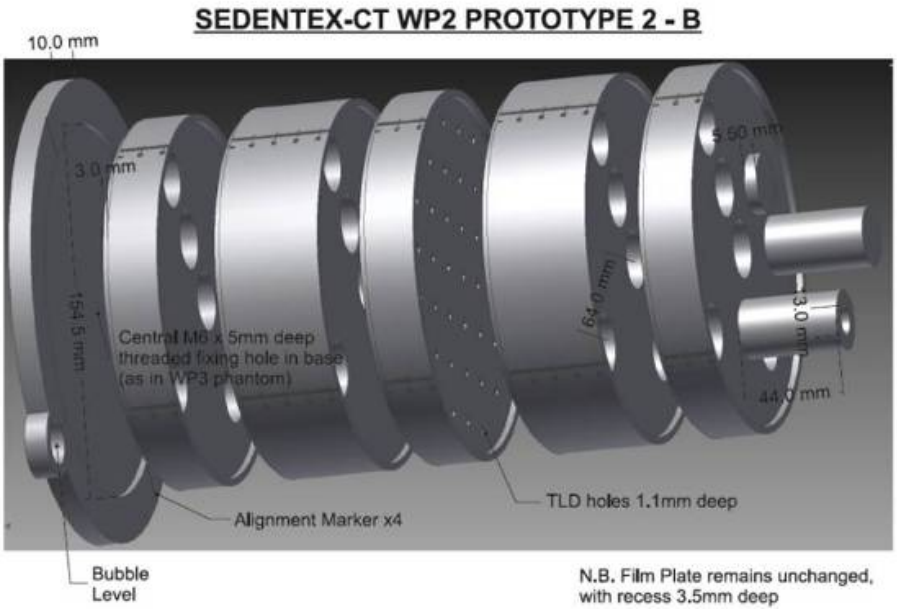

Figure 1. Phantom for dose index validation, containing holes at different locations and insert to fill up unused holes

The phantom was scanned on two CBCT devices: 3D Accuitomo 170 (J. Morita, Kyoto, Japan) and Scanora 3D (Soredex, Tuusula, Finland), involving a vast amount of exposure protocols, varying all possible exposure factors (FOV size, kVp, mAs, rotation arc). Two types of ion chambers were used: a 0.6 cm^3 chamber (Farmer FC65-G, IBA Dosimetry, Schwarzenbruck, Germany), which was calibrated in a RQR5 diagnostic beam, and a 6 cm^3 thimble ionisation chamber (Radcal 9010, Radcal Corporation, California, USA) coupled with an electrometer (Radcal 9010, Radcal Corporation, California, USA) with calibration traceable to national standards (National Physical Laboratory). An intercomparison was performed to ensure consistency in measurements between the two centres.

Two indices were measured for all involved exposure protocols. Figure 2 shows an axial drawing of the phantom with the different possible measuring positions. Index 1 was measured by combining points 4B, 3B, 2B, 1, 2F, 3F and 4F *i.e.* seven measuring points along the diameter of the phantom. Index 2 was measured using point 1, 4B, 4R, 4F, and 4L *i.e.* five measuring points in the center and along the border of the phantom.

For the third proposed index from D2.1 (the dose-area-product, DAP), no measurements were obtained in addition to those incorporated into D2.1.

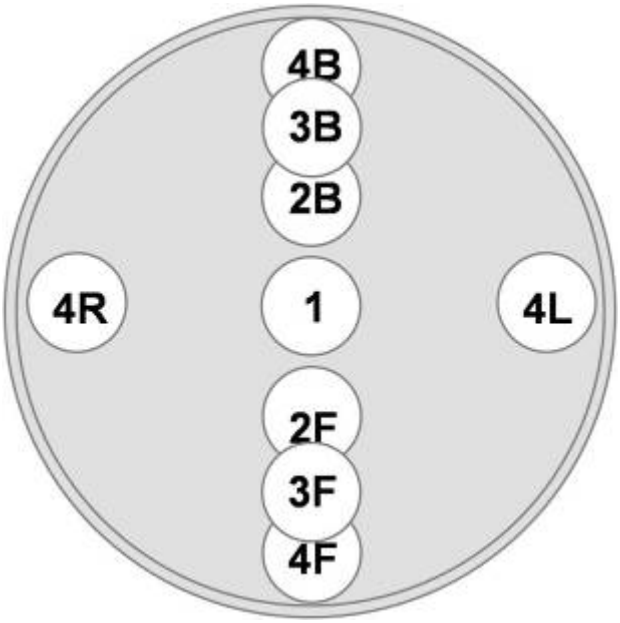

Figure 2. Nine possible measuring points on the phantom. F = front, B = back, R = right, L = left

4.3 Modelling of dental CBCT

In this study, modelling of the radiation transport was done using Monte Carlo simulation. Monte Carlo methods are a class of computational algorithms that are based on repeated random sampling to compute their results. It offers a flexible but rigorous approach toward photon propagation in human tissues. The local rules of radiation transport are expressed as probability distributions which describe the photon movement between interaction points. The probability density functions are sampled using random sampling which models the outcome of physical events like photon collisions, photon energies, scattering angles, etc. The simulation can score multiple physical quantities simultaneously and it relies on calculating the transport of a large number of photons because it is statistical in nature.

Monte Carlo N-Particle (MCNP) code, which was used in this study, is a general-purpose Monte Carlo code which is widely used in radiation protection and medical physics [http://mcnp-green.lanl.gov/]. In this study, the latest version (v5) was used. The simulations were performed on a cluster of 32 processors and the processing time ranged from a few minutes to several hours depending on the geometry and the number of photons/histories.

4.3.1 Cone beam geometry

A dental CBCT scanner utilises a conventional X-ray tube coupled to a flat panel detector or an image intensifier. The x-ray tube rotates around a fixed point in space, known as isocentre. The dimensions of the radiation field, also known as field of view (FOV), are defined at the isocentre. The FOV varies

from small sizes such as 4cmØ x 3cm to large sizes such as 20.6cmØ x 18.4cm. There is a wide range of filtrations and tube voltages utilised by the scanners ranging from 2.1mm Al to 14.6mm Al and from 60kVp to 120kVp.

The cone beam CT source was modelled using a number of stationery point x-ray sources with biased direction toward the isocentre. The sources were placed at a circle with a radius equal to the distance between the focal spot and the isocentre and at 10° intervals. The radiation field was shaped to the desired dimensions with the use of horizontal and vertical collimators. The X-ray spectra were generated using the SRS-78 Spectrum Processor [Cranley *et al*].

The distance between the point sources and the isocentre, the number of sources and the rotation arc, the FOV, the X-ray spectra and the position of the isocentre in the computational phantoms were adjusted according to the CBCT scanner and the exposure conditions.

4.3.2 Computational phantoms

PMMA computational phantom

A poly(methyl methacrylate) (PMMA) phantom of 16cmØ x 20cm, which was designed and used for the determination of the dose index in Deliverable 2.1, was modelled as the first stage of the model validation.

10 year old ATOM voxel phantom

The 10 year old phantom which was used for the anthropomorphic measurements was modelled for the second stage of the validation and for calculating the conversion factors to effective dose for a paediatric reference patient as there are no publicly available computational phantoms.

The phantom was scanned on a Philips Brilliance Big Bore CT scanner (Queen Elizabeth hospital, Birmingham). The head and neck sections of the ATOM phantom consist of bone, soft tissue and air. A MATLAB routine was written to convert the pixel values of bone, soft tissue and air of the CT images to three arbitrary numbers that were assigned to the three materials. The positions of the TLDs were modelled as air cavities in the voxel model. The voxel size was 1.14mm x 1.14mm x 5mm. Once the matrix was developed, it was inserted in the CBCT geometry. The dose to the three tissues was calculated using the F6, energy deposited per gram per source particle, tally.

Adult male voxel phantoms

The ICRP publication 110 describes the development and intended use of the Reference Male and Female computational phantoms. The adult male ICRP reference computational phantom was used to calculate the conversion factors to effective dose for a typical adult male patient.

The ICRP male reference computational phantom was constructed using the whole-body CT slices of a 38-year-old individual with a height of 176cm and a mass of 70kg. The resolution of the computational phantom was 2.137mm x 2.137mm x 8mm. A list of tissues and their elemental composition is provided in the ICRP publication.

A routine in MATLAB was written to extract the slices 185 to 222, from the bottom slice of the thyroid to the top skin slice. In total, 54 individual tissues were modelled but the dose was calculated only for the radiosensitive organs in the head and neck region which are the red bone marrow, endosteum, salivary glands, thyroid, anterior nasal passage, posterior nasal passage, oral mucosa, brain, lymph nodes, muscle, skin and oesophagus. The dose to all the radiosensitive organs in the head and neck region were calculated with the exception of oesophagus and skin. From the anthropomorphic phantom dose measurements, it was found that the contribution of the oesophagus and skin to the effective dose were less than 1% and therefore, the doses to these organs were not calculated.

Relevant bones to dental CBCT are the mandible, cervical spine, thoracic spine, ribs, clavicles, cranium, upper halves of humeri and scapulae. Only the dose to the red bone marrow located in the cervical spine, cranium and mandible was calculated, since the dose to the red marrow for the rest of the bones was very small. The endosteum dose was calculated from the average spongiosa doses to the cervical spine, mandible and cranium weighted for the endosteum content to each of the three bones [Zankl et al]. The dose to the red bone marrow was calculated following the methods of King and Spiers, Liu et al and Zankl et al studies.

The F6, energy deposited per gram per source particle, tally was used to estimate the dose to the radiosensitive organs and the F4, energy fluence per source particle, tally was used to calculate the energy fluences for the different bones and slices.

4.3.3 Validation of the models and conversion factors

The first stage of the validation was to compare the calculated doses of the modelled PMMA geometry with the measured doses using TLDs. The PMMA measurements are described in detail in deliverable report D2.1. All measurements were done on a 3D Accuitomo 170 (J. Morita, Kyoto, Japan) machine (Manchester, UK). The machine was modelled using the filtration, anode angle, focus to isocentre distance and collimator set up, referenced in the technical manual.

Since the F6 tally calculates the dose per source particle, the calculated doses per source particle values were normalised to the absorbed dose per source particle that was deposited at the centre of the phantom. The TLD measured doses were normalised to the mAs and to the TLD dose at the centre of the PMMA phantom to allow a direct intercomparison between

measured and calculated doses. Simulated and measured data were compared for a range of tube voltages, FOVs, rotation arcs and positions of the isocentre.

The second stage of the validation was to compare the effective doses calculated using the modelled 10 year old ATOM phantom with the measured effective doses. Measured and simulated effective dose/mAs were compared for a range of CBCT machines, FOVs, tube voltages and imaging protocols.

The conversion factors were calculated for both the 10 year old ATOM phantom and the ICRP male reference computation phantom for ten CBCT machines and for a range of FOVs, tube voltages and imaging protocols. For the medium and large FOVs, the bottom edge of the radiation field was aligned with the bottom of the mandible and the front edge was aligned with the tip of the nose. For small FOVs, the isocentre was placed at the tooth under investigation.

4.4 Relationship between conversion factors and dose index

The relationship between the conversion factors and the two proposed dose indices was investigated using the measurements on the Accuitomo 170 machine and the conversion factors calculated using the Monte Carlo code. The relationship between the dose indices, the irradiated volume and the conversion factors was investigated.

5. Results

5.1 Measurements using anthropomorphic phantoms

The following results were published in Pauwels *et al*, European Journal of Radiology, 2011 (Epub 2010).

Table 3 gives the absorbed organ doses and effective dose for large FOV protocols for the adult phantom. The effective dose ranged between 68 and 368 μSv. The highest absorbed dose was in the salivary glands, although the largest contribution to the effective dose was provided by the remainder tissue due to its higher weighting factor.

Table 3. Absorbed organ doses (μGy) and effective dose (μSv) for large FOV (maxillofacial) protocols

	Galileos	i-CAT N.G.	Iluma	Kodak 9500	NewTom VG	NewTom VGi	Scanora 3D	SkyView
Red bone marrow	82	116	660	206	115	186	86	134
Thyroid	380	355	1230	585	354	2045	296	474
Skin	55	54	277	92	50	98	55	58
Bone surface	83	124	667	215	163	184	94	125
Salivary glands	2104	1830	7225	2676	1690	2855	1568	1582
Brain	124	375	3415	1205	251	605	255	719
Remainder	292	260	1034	380	281	436	221	224
Effective dose	84	83	368	136	83	194	68	87

Adult dose measurements for medium FOV protocols are shown in Table 4, showing effective doses between 28 and 265 μSv. Compared with the results for the large field protocols, organ doses were distributed similarly, although it is seen that the contribution of the brain was lower.

Table 5 shows the results for the small FOV protocols. The effective dose ranged between 19 and 44 μSv. From these results, the effect of FOV positioning can be observed. Comparing an upper jaw, frontal region with a lower jaw, molar region scan from the Kodak 9000 3D, it is seen that there were large differences regarding the absorbed dose for the salivary glands, thyroid gland, oral mucosa and extrathoracic airways.

Table 4. Absorbed organ doses (μGy) and effective dose (μGy) for medium FOV (dentoalveolar or single jaw) protocols

	3D Accuitomo 170	i-CAT N.G.	Kodak 9500	NewTom VGi	Picasso Trio	Picasso Trio	ProMax 3D	ProMax 3D	Scanora 3D	Scanora 3D	Scanora 3D	Veraviewepocs 3D
Protocol[a]	upper jaw				high dose	low dose	high dose	low dose	upper jaw	lower jaw	both jaws	
Red bone marrow	112	33	85	294	126	62	88	27	42	34	37	55
Thyroid	148	251	541	1293	551	583	1021	202	148	352	240	330
Skin	62	25	51	145	113	56	145	15	30	29	31	69
Bone surface	112	33	84	299	156	57	121	26	50	35	39	57
Salivary glands	2138	973	2166	6372	2982	1837	2576	596	1285	1052	1117	1956
Brain	189	46	91	431	134	39	53	28	45	25	31	40
Remainder	85	172	304	881	432	254	346	83	178	147	155	267
Effective dose	54	45	92	265	123	81	122	28	46	47	45	73

[a] *If not specified, the positioning of the FOV is dentoalveolar (both jaws)*

Table 5. Absorbed organ doses (µGy) and effective dose (µSv) for small FOV (localised) protocols

	3D Accuitomo 170	Kodak 9000 3D	Kodak 9000 3D	Pax-Uni3D
FOV positioning	Lower jaw, molar region	Upper jaw, front region	Lower jaw, molar region	Upper jaw, front region
Red bone marrow	37	21	78	47
Thyroid	195	30	251	209
Skin	32	25	24	55
Bone surface	37	27	35	49
Salivary glands	2120	523	709	1073
Brain	37	18	290	28
Remainder	70	74	86	146
Effective dose	43	19	40	44

The average effective doses for all devices for each FOV group are shown in Figure 3. The average doses for large, medium and small FOVs were 131, 88 and 34 µSv respectively. The standard deviations were 91 (70% of mean), 70 (83%) and 14 (37%), showing large variability of doses for large and medium FOV groups.

Figure 4 illustrates the average contribution of each of the measured organs to the effective dose. The remainder organs have the highest contribution, followed by the salivary glands and thyroid gland. Contributions of brain, bone surface and skin are almost negligible. No notable differences were seen when comparing the contributions for small, medium and large FOVs separately.

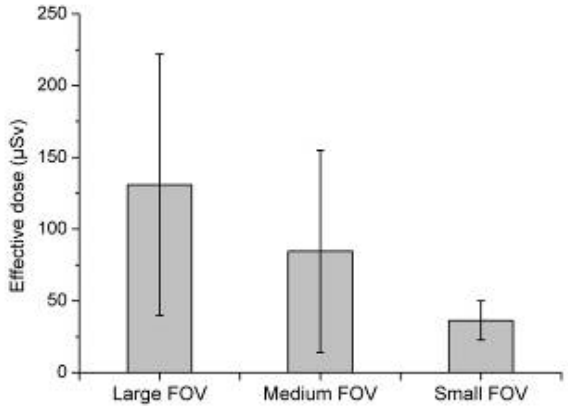

Figure 3. Average effective dose for CBCT devices, divided into groups based on field of view size. Standard deviations are shown for each group.

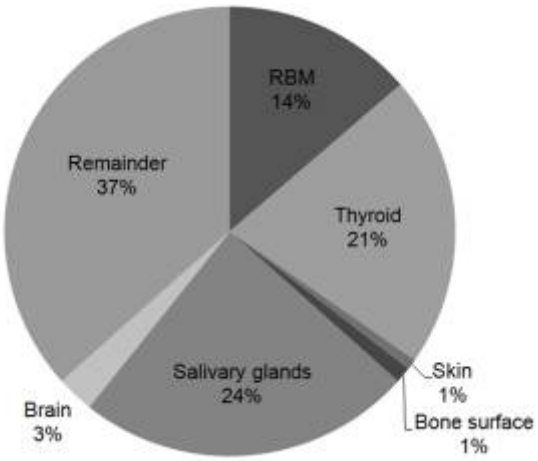

Figure 4. Average contribution of organs to effective dose.

The following results were published in Theodorakou *et al*, British Journal of Radiology, in press.

Tables 6 and 7 show the effective dose for the adolescent and 10 year old phantom, respectively. The average effective doses for all CBCT devices for the adolescent and for the 10 year old phantoms were 111μSv and 151μSv respectively. These averages are well below the values for MSCT, but considerably higher than those for panoramic and cephalometric radiography. The minimum effective dose for the ten year old was 16μSv and for the adolescent 18μSv and the maximum effective doses for the adolescent and 10 year old were 578μSv and 735μSv respectively.

Table 6. Effective dose for the adolescent phantom (ATOM model 702-C)

Device	Protocol	Effective dose (μSv)
3D Accuitomo 170	17x12cm	216
3D Accuitomo 170	14x10cm	186
3D Accuitomo 170	14x5cm, Maxilla	70
3D Accuitomo 170	4x4cm, Wisdom, Maxilla	32
Galileos		71
i-CAT N.G.	6cm mandible	49
i-CAT N.G.	6cm maxilla	33
i-CAT N.G.	13cm portrait	82
Kodak 9000 3D		24
NewTom VG	dental	81
ProMax 3D		18
ProMax 3D MAX		578
Scanora large FOV		74
Scanora medium FOV		52
SkyView		90
Somatom Sensation 64		1047
Veraviewepocs 2D	Panoramic	6,4
Veraviewepocs 2D	Cephalometric	1

Table 7. Effective dose for the 10 year old phantom (ATOM model 702-C)

Device	Protocol	Effective dose (μSv)
3D Accuitomo 170	17x12cm	282
3D Accuitomo 170	14x10cm	237
3D Accuitomo 170	14x5cm, Mandible	215
3D Accuitomo 170	4x4cm, Impacted canine, Maxilla	28
Galileos		70
i-CAT N.G.	6cm mandible	63
i-CAT N.G.	6cm maxilla	43
i-CAT N.G.	13cm portrait	134
Kodak 9000 3D		16
NewTom VG	dental	114
ProMax 3D		24
ProMax 3D MAX		735
Scanora large FOV		85
Scanora medium FOV		67
SkyView		105
Somatom Sensation 64		605
Veraviewepocs 2D	Panoramic	10
Veraviewepocs 2D ceph	Cephalometric	2

5.2 Dose index validation measurements

As this is a public deliverable, no detailed results can be provided, as these are still awaiting submission/publication. It can be seen that both indices are affected by the amount of exposure and geometric factors (FOV size and

position). Generally, there is a good consistency between the two indices; the largest differences are seen for 180° scans, as they show the largest dose gradients.

5.3 Monte Carlo simulations and conversion factors

Validation of the Monte Carlo models

The cone beam geometry and the modelled computational phantoms were validated in two stages. The first stage compared the calculated with measured doses by modelling a PMMA cylinder on a 3D Accuitomo 170 CBCT scanner. The % difference between the calculated and measured normalised doses ranged between 7% and 20%. The percentage error in the TLD measurements was less than 10%.

The second stage of validation compared the calculated with measured normalised doses by modelling the 10 year old ATOM phantom on three CBCT scanners for a range of FOVs, tube voltages and imaging protocols. The percentage difference between measured and calculated effective doses ranged from 3% to 17%.

Conversion factors

Tables 8 and 9 show examples of the calculated conversion factors in mSv/mAs for the 10 year old ATOM phantom and the ICRP male reference male phantoms. In order to convert to effective dose, the conversion factor should be multiplied by the mAs used.

Table 8. Conversion factors (mSv/mAs) for the 10 year old ATOM phantom

CBCT machine	Field of view (cm^2)	Tube voltage	Rotation (degrees)	Conversion factor
iCAT NG	16cmØx6cm Mandible	120	360	0.00333
NewTom 5G	15cmØx12	110	360	0.00221
NewTom VGi	15cmØx15cm	110	360	0.00626
3D Accuitomo 170	17cmØx12cm	90	180	0.00348

Table 9. Conversion factors (mSv/mAs) for the ICRP male reference computational phantom

CBCT machine	Field of view (cm^2)	Tube voltage	Rotation (degrees)	Conversion factor
iCAT NG	16cmØx6cm Maxilla	120	360	0.00130
NewTom VGi	12cmØx7.5cm Mandible	110	360	0.00249
NewTom 5G	15cmØx12cm	110	360	0.00129
3D Accuitomo 170	17cmØx5cm Mandible	90	360	0.00126

It should be noted that an intercomparison between machines based on the above list of conversion factors should not be made because the mAs may vary from machine to machine and the image quality has not been assessed in this study.

The conversion factors between the two phantoms for the same settings are different because of the different size, shape and composition of the two phantoms.

5.4 Relationship between conversion factors and dose index

The conversion factors that are presented in this report are CBCT machine specific and convert between the used mAs and the effective dose. If the physical starting quantity for the conversion would contain more dose information than merely the impact on the dose of the mAs, the conversion factors are expected to be more generic. A good candidate for such a physical starting quantity would be the dose index. Therefore, the relationship between the dose indices and the MCNP conversion factors was investigated for both the ICRP reference male and the 10 year old ATOM phantom. In particular, a correlation was found between the conversion factors and the dose indices normalised to the mAs. These results will be analysed in more detail in order to determine the underlying physical model. Another interesting result of analysing the dose indices is that the value of the dose index is mainly determined by the mAs and the irradiated volume.

Normalised dose index 2 to the mAs and irradiated volume showed a smaller variation across the irradiated volumes than normalised dose index 1. It was found that the dose index 2 correlates better with the conversion factors. A linear relationship between the dose indices and the conversion factors was established.

6. Work in the final period: Conclusions

6.1 Anthropomorphic equivalent phantom measurements

The absorbed organ doses and effective dose were estimated using adult and paediatric phantoms involving a large number of CBCT devices, applying exposure protocols with wide ranges for exposure parameters such as kVp, mAs and FOV size.

For adult and paediatric phantoms, the results show the wide range of doses existing for CBCT imaging. For many devices, the effective dose was found to be below 100µSv; for some devices the effective dose was considerable higher due to a combination of a large FOV (covering all radiosensitive organs in the head) and a high exposure.

It is clear that different devices can have other application ranges based on the available FOV size(s). Those devices that allow the option to scan with FOVs of a few cm^3 can be used for localised problems (e.g. endodontic problem) whereas other devices are not optimised for these particular applications, as they have a much larger FOV and typically acquire both dental arches or even the entire dentomaxillofacial area in a single scan, and can therefore be applied for orthodontic cases, ENT patients or maxillofacial surgery. Some devices allow for a wide range of FOV sizes, broadening their application range.

The influence of kVp and mAs on the dose is clear as well, although these parameters should be interpreted more carefully, as they affect the image quality. For example, scans using a higher mAs can be reconstructed using a smaller voxel size and thus a higher spatial resolution. The most optimal situation in terms of patient dose optimisation is where the user can select these parameters based on the required image quality. For example, small endodontic problems such as root fractures require a high degree of spatial and contrast resolution, whereas implant planning has a lower standard of image quality.

A final conclusion based on the effective dose measurements is that the dose for paediatric patients can be considerably higher than for adults if the same exposure parameters are applied. Furthermore, children are more sensitive for stochastic effects, leading to a multiplication of the risk for young patients. This is an important finding, as it is seen in practice that CBCT is routinely applied to children for maxillofacial and orthodontic problems, which used to be addressed using conventional imaging. Whereas MSCT was avoided as much as possible due to its high dose, the introduction of CBCT has led to the increasing use of 3D imaging for paediatric cases, increasing the collective dose for children. It is pivotal that these children can be scanned using the lowest possible dose, ideally by allowing for the adjustment of exposure parameters (*e.g.* lowering the mAs).

6.2 Dose index validations measurements

The two dose indices defined in deliverable D2.1 were measured in practice using a customized phantom and small-volume ionisation chambers. These measurements were limited to two CBCT devices, as these devices allow for a wide range of exposure geometries (FOV sizes between 4x4cm and 17x12 cm, 180° and 360° rotation) allowing for the assessment of the indices for a large number of protocols.

The results show the effect of the size and positioning of the FOV on the index. For large FOVs, all measurements are within the primary beam for all exposure angles. For smaller FOVs or partial rotations, part of the measurements fall outside the primary beam for part of the exposure, showing a significant decrease in dose and resulting in a lower value for the dose index.

The measurements show that the indices can be measured routinely in practice, providing that the right tools are available, and that they are sensitive to changes in exposure factors. However, for a true validation, these indices had to be compared to the effective dose. This is described in the following subsection.

6.3 Conversion factors and the relationship between conversion factors and dose index

The conversion factors (mSv/mAs) from mAs to effective dose for an adult and paediatric computational phantom were calculated for a range of dental CBCT machines and clinical examinations. The error in the computational models was quantified in two stages and it was found to be less than 17%. The conversion factors increase as the irradiated volume increases due to the higher amount of scattered radiation. In addition, the conversion factors increase as the tube voltage and the filtration increase.

The conversion factors verify the general trend that was found with the anthropomorphic phantom dose measurements, that the closer the isocentre is to the salivary glands and thyroid, the higher the dose and the conversion factors are.

The relationship between the two proposed dose indices and the exposure factors was investigated using the validation dose index measurements. It was found that dose index 2 normalised to the mAs and to the logarithm of the irradiated volume is independent of the rotation arc and of the irradiated volume. Thus, an average value of dose index 2 normalised to the mAs and to the logarithm of the irradiated volume was calculated. This average can be used to convert to dose index 2 when multiplied by the used mAs and irradiated volume. Dose index 2 was measured using five measurements, one

at the centre and four at the periphery. Additional measurements should be done to establish how the number and location of dose measurements affect the relationship between the dose index, irradiated volume and rotation arc.

The relationship between the conversion factors and the two dose indices was investigated for the two computational phantoms and a correlation was found. The relationship is however empirical and further work should be done using the Monte Carlo simulations and additional dose index measurements to investigate the physical principles behind it.

7. Overall Work Package Conclusions

This section considers both the earlier work and the work in the final period, to draw conclusions regarding the SEDENTEXCT Guidelines and the overall impact of the work, and to summarise the implications for further work.

7.1 SEDENTEXCT Guidelines

As seen in the draft Guidelines for the use of CBCT, defined in collaboration with the European Academy of Dental and Maxillofacial Radiology (EADMFR), dose optimisation is one of the cornerstones in the list of basic principles (Horner *et al*). Apart from general principles that are applied for all uses of ionising radiation, such as the justification of exposure, there are a few specific principles which are supported by the results from WP2. The results obtained in the final part of WP2 can lead to a further fine-tuning of these principles.

The first principle is the limitation of the FOV size to the clinical situation. There is a wide array of clinical applications of CBCT imaging, with variable needs of regions of interest size, ranging from a single root to the entire dentomaxillofacial area. The dose estimations performed in WP2 show the vast range of organ or effective doses, implying that large-, medium- and small-volume devices should be evaluated separately, as they should be applied to different patient groups. Ideally, any CBCT device should allow for different FOV choices based on the clinical situation.

The second principle is the adjustment of other exposure parameters based on the clinical situation. Based on image quality requirements, the user should be allowed the freedom to choose the most appropriate imaging parameters that allow for a clinical assessment at the lowest achievable exposure.

A more specific principle, related to the previous one, is that devices should contain a ‘low-dose’ exposure which can be used for paediatric cases. As dose optimisation is crucial for children, and lower doses can be applied to them without hampering image quality, it should be possible to select lower dose levels for children compared to adult cases.

Also, the need for acceptance testing and quality control is addressed by the results from WP2, as different dose indices were defined that can be applied in practice to assess the device’s exposure over time, and to estimate patient dose in a practical way.

Finally, by measuring the scatter dose, the risk for personnel was assessed, showing the need for an appropriate installation of the device in the clinical environment.

7.2 Impact

Apart from the incorporation of its results in the SEDENTEXCT Guidelines, WP2 is expected to have a significant impact on the research community, clinical users of CBCT and CBCT manufacturers.

A few major gaps in literature were addressed. A thorough assessment of the effective dose range for CBCT was performed, and paediatric phantoms were used to estimate the radiation risk for children. Skin measurements were performed to assess the variability of absorbed dose for different patient groups. By investigating the dose distribution in homogeneous phantoms, dose indices were defined which can be measured in routine practice and converted to effective dose. Personnel protection was addressed by measuring scatter dose.

The objectives of WP2 were (1) to develop a method to readily characterise the dose distribution for different scanners, using measurements simply performed in the field, to allow simple conversion to effective dose, and (2) to determine the scatter dose distribution around scanners and explore the consequences for operator dose. Both objectives were met and are in the process of being disseminated to the public. To this date, the impact of the work performed in WP2 was provided by dissemination in terms of presentation at international (radiology and medical physics) congresses and meetings, and the publication of two papers containing the effective doses for adult and paediatric phantoms. In the near future, the different tasks in WP2 will be further disseminated (see subsection 7.4).

It is expected that the dose indices defined in WP2 will be incorporated into practice and lead to a standardisation of the measurement of CBCT exposures. Furthermore, the results will lead to an optimisation of patient and personnel doses by adhering to the principles defined in the SEDENTEXCT Guidelines.

There has been one change to the DoW that needs to be mentioned, although it did not affect the outcome or impact of WP2. We proposed to omit the originally planned second approach in WP2.4, which is the use of a commercial radiotherapy planning system (Pinnacle). It was felt that the experimental work by KUL would be of much higher value to the project if it would be oriented towards the validation of the dose indices instead of performing parallel simulation work, which would in essence only confirm the Monte Carlo simulations, and would as such be of second order importance to the project.

7.3 Roadmap

Although WP2 provides a vast amount of dosimetric data, it also provides the opportunity for future scientific work, seeing that a few topics could not be part of the project's scope.

First of all, the dosimetric methods applied in WP2 (accurate measurement of effective dose, measurement of dose index, Monte Carlo simulation of dose) can be applied to new CBCT devices to investigate their performance in terms of radiation exposure. This can aid manufacturers in the optimisation of their devices in concordance with the SEDENTEXCT Guidelines.

Furthermore, the organ and effective doses measured can generally be considered low in terms of cancer risk, and the actual risk for stochastic effects for these low doses has been debated. The doses measured can provide input for specific research on the added cancer risk of dental CBCT examinations.

7.4 Future dissemination

The different tasks in WP2 will be further disseminated by means of a number of papers and additional presentations at international conferences and meetings. An important dissemination will be provided by the final SEDENTEXCT Guidelines, for which all WP2 tasks provide input.

8. References

Brenner DJ. It is time to retire the computed tomography dose index (CTDI) for CT quality assurance and dose optimization. For the proposition. Med Phys 2006;33:1189-90.

Cohnen M, Kemper J, Möbes O, Pawelzik J, Mödder U. Radiation dose in dental radiology. Eur Radiol 2002;12:634-7.

K Cranley, B J Gilmore, G W A Fogarty and L Desponds. Catalogue of diagnostic X-ray spectra and other data Institute of Physics in Medicine and Engineering, 1997.

Dixon RL. A new look at CT dose measurement: beyond CTDI. Med Phys 2003;30:1272-80.

Dixon RL. Restructuring CT dosimetry--a realistic strategy for the future Requiem for the pencil chamber. Med Phys 2006;33:3973-6.

Dixon RL, Boone JM. Cone beam CT dosimetry: a unified and self-consistent approach including all scan modalities--with or without phantom motion. Med Phys 2010;37:2703-18.

Fearon T. CT dose parameters and their limitations. Pediatr Radiol 2002;32:246-9.

Hirsch E, Wolf U, Heinicke F, Silva MA. Dosimetry of the cone beam computed tomography Veraviewepocs 3D compared with the 3D Accuitomo in different fields of view. Dentomaxillofac Radiol 2008;37:268-73.

Horner K, Islam M, Flygare L, Tsiklakis K, Whaites E. Basic principles for use of dental cone beam CT: consensus guidelines of the European Academy of Dental and Maxillofacial Radiology. Dentomaxillofac Radiol 2009;38:187-95.

International Commission on Radiological Protection. Recommendations of the International Commission on Radiological Protection. ICRP Publication 26. Ann ICRP 1(3). Oxford, UK: Pergamon Press, 1978.

International Commission on Radiological Protection. Recommendations of the International Commission on Radiological Protection. ICRP Publication 103. Ann ICRP 37. Oxford, UK: Pergamon Press, 2007.

International Commission on Radiological Protection. Reference Man: Anatomical, physiological and Metabolic Characteristics. ICRP Publication 23. Pergamon Press, 1975.

International Commission on Radiological Protection: Adult reference computational phantoms. ICRP Publication 110. Pergamon Press, 2009.

International Commission on Radiological Protection: Basic Anatomical and Physiological Data for Use in Radiological Protection: Reference Values. ICRP Publication 89. Pergamon Press, 2003.

Jessen KA, Shrimpton PC, Geleijns J, Panzer W, Tosi G. Dosimetry for optimisation of patient protection in computed tomography. Appl Radiat Isot 1999;50:165-72.

King SD and Spiers FW. Photoelectron enhancement of the absorbed dose from X-rays to human bone marrow: experimental and theoretical studies. The British Journal of Radiology 58, 345-356.

Liye Liu, Zhi Zeng, Junli Li, Binquan Zhang, Rui Qiu and Jizeng Ma An ICRP-based Chinese adult male voxel model and its absorbed dose for idealized photon exposures—the skeleton. Phys Med Biol 54 6675-6690.

Lofthag-Hansen S, Thilander-Klang A, Ekestubbe A, Helmrot E, Gröndahl K. Calculating effective dose on a cone beam computed tomography device: 3D Accuitomo and 3D Accuitomo FPD. Dentomaxillofac Radiol 2008;37:72-9.

Loubele M, Bogaerts R, Van Dijck E, Pauwels R, Vanheusden S, Suetens P, et al. Comparison between effective radiation dose of CBCT and MSCT scanners for dentomaxillofacial applications. Eur J Radiol 2009;71:461-8.

Ludlow JB, Davies-Ludlow LE, Brooks SL and Howerton WB. Dosimetry of 3 CBCT devices for oral and maxillofacial radiology: CB Mercuray, NewTom 3G and i-CAT NG. Dentomaxillofac Radiol 2006;35:219-226.

Ludlow JB, Ivanovic M. Comparative dosimetry of dental CBCT devices and 64-slice CT for oral and maxillofacial radiology. Oral Surg Oral Med Oral Pathol Oral Radiol Endod 2008;106:106-14.

Mah JK, Danforth RA, Bumann A, Hatcher D. Radiation absorbed in maxillofacial imaging with a new dental computed tomography device. Oral Surg Oral Med Oral Pathol Oral Radiol Endod 2003;96:508-13.

Mori S, Endo M, Nishizawa K, Tsunoo T, Aoyama T, Fujiwara H, et al. Enlarged longitudinal dose profiles in cone-beam CT and the need for modified dosimetry. Med Phys 2005;32:1061-9.

Nakonechny KD, Fallone BG, Rathee S. Novel methods of measuring single scan dose profiles and cumulative dose in CT. Med Phys 2005;32:98-109.

Okano T, Harata Y, Sugihara Y, Sakaino R, Tsuchida R, Iwai K, et al. Absorbed and effective doses from cone beam volumetric imaging for implant planning. Dentomaxillofac Radiol 2009;38:79-85.

Perisinakis K, Damilakis J, Tzedakis A, Papadakis A, Theocharopoulos N, Gourtsoyiannis N. Determination of the weighted CT dose index in modern multi-detector CT scanners. Phys Med Biol 2007;52:6485-95.

Roberts JA, Drage NA, Davies J, Thomas DW. Effective dose from cone beam CT examinations in dentistry. Br J Radiol 2009;82:35-40.

Silva MA, Wolf U, Heinicke F, Bumann A, Visser H, Hirsch E. Cone-beam computed tomography for routine orthodontic treatment planning: a radiation dose evaluation. Am J Orthod Dentofacial Orthop 2008;133:640.e1-5.

Suomalainen A, Kiljunen T, Käser Y, Peltola J, Kortesniemi M. Dosimetry and image quality of four dental cone beam computed tomography scanners compared with multislice computed tomography scanners. Dentomaxillofac Radiol 2009;38:367-78.

Tsiklakis K, Donta C, Gavala S, Karayianni K, Kamenopoulou V, Hourdakis CJ. Dose reduction in maxillofacial imaging using low dose Cone Beam CT. Eur J Radiol 2005;56:413-7.

M Zankl, U Fill, N Petoussi-Henss and D Regulla Organ dose conversion coefficients for external photon irradiation of male and female voxel models Phys Med Bio 47(14); 2367-2385, 2002.

http://mcnp-green.lanl.gov/

http://www.nist.gov/pml/data/xraycoef/index.cfm


EUROPEAN COMMISSION
European Research Area